

THERMOELECTRIC WASTE HEAT RECOVERY OF AN AUTOMOTIVE INTERNAL COMBUSTION ENGINE USING (Na, K) CO-DOPED POLYCRYSTALLINE TIN SELENIDE (SnSe)

by

**Muhammad Irfan KHAN^{a,b}, Ali Hussain KAZIM^a,
Ghulam Moeen UDDIN^a, Jawad SARWAR^a, Muhammad FAROOQ^a,
Muhammad Rohail DANISHⁱ and Aqsa SHABBIR^{c*}**

^a Department of Mechanical Engineering, University of Engineering and Technology,
Lahore, Pakistan

^b Lahore School of Aviation, The University of Lahore, Lahore, Pakistan

^c Department of Electrical Engineering, Lahore College for Women University, Lahore, Pakistan

Original scientific paper

<https://doi.org/10.2298/TSCI200620300K>

Recent developments in converting the thermal energy of exhaust gasses of automobiles into electric power directly, require an extensive simulation and design of appropriate TEG system. This work aims to create a physical model of engine exhaust system using Simscape language to simulate waste heat recovery from the exhaust gasses using (Na, K) co-doped polycrystalline tin selenide, SnSe, TE material. This particular material exhibits a high Seebeck coefficient and extremely low lattice thermal conductivity in power generation because of phonons scattering by the rattlers (Na, K atoms) and nanostructuring. In the MATLAB/SIMULINK environment, a transient simulation is done for the recovery of waste heat from a 1.5 liters engine using these specific material-based TE modules. According to the results obtained, at the temperature gradient of 285 K across its sides, electrical power of 10.4 W with a conversion efficiency of almost 5% is produced from one module. The total system output power was 477 W at the exhaust gas inlet temperature of 900 K to the octagonal HEx on which the modules are mounted.

Key words: co-doped polycrystalline SnSe, IC engines, TE devices, waste heat recovery

Introduction

From the invention of the very first and basic IC (IC) engine to the current advanced one, as much as 65% of usable thermal energy is being lost to the environment [1]. This tremendous percentage of wasted thermal energy is due to Carnot's limitations and also due to the less efficient conversion of other inevitable processes [2]. Such losses not only decrease the thermal efficiency of the engine but also increase the percentage of greenhouse and other harmful gasses for a specified output power of a particular engine. However, due to the inflation of fuel prices and the depletion of these non-renewable energy resources, there is an urgent need for the automotive industry to reduce these losses and use this thermal energy wisely and efficiently [3].

* Corresponding author, e-mail: aqsa_shabbir@outlook.com

The literature has presented that a viable way to improve thermal efficiency, reduce specific fuel consumption, and reduce the GHG of an IC engine for given output power is to recover the thermal energy that is being wasted in the exhaust gases [4]. Shu *et al.* [5] experimentally demonstrated that a lot of thermal energy contained by the exhaust gasses is wasted in the atmosphere. Jorge *et al.* [6] have shown that the engine's fuel consumption is reduced by 10% if 6% of the total exhaust heat is recovered into the electricity production.

Several waste heat recovery technologies were studied and investigated *i. e.* exhaust gas recirculation [7], turbocompounding systems (turbocharging and supercharging) [8], thermodynamic cycles (Rankine, Stirling, Ericsson, *etc.*), and thermoacoustic systems [9]. However, to transform the low-grade waste heat of an automotive IC engine directly into high-grade electrical energy, a promising technology called thermoelectric (TE) technology has been an important area of research for both academia and industry over the last three decades [10-13].

This technology holds significant merits due to its quiet, environmentally friendly, and maintenance-free operation. Moreover, these TE devices have no moving parts along with minimal vibrations and have a long-life span compared to the others [14]. However, because of their lower power conversion efficiency and the cost of material being a little bit higher, these devices are still not extensively used. Consequently, both academia and industry have placed a great deal of effort in recent years to find TE materials with higher power conversion efficiency and at the same time low cost, which will be a promising solution to the aforementioned problems [15, 16].

Thermoelectricity is the branch of solid-state physics which deals with the direct conversion of electricity based on the fact that charge carriers travel from one side of a material to the other side employing temperature gradient [17]. Generally, two physical phenomena are discussed in this branch and the Seebeck effect and the Peltier effect as described in [18, 19]. The Seebeck effect states that an open circuit voltage is produced in the TE material as long as the temperature gradient exists across it. The Seebeck coefficient or thermopower, S , is a material property that relates open circuit voltage V_{oc} with the temperature gradient ΔT given:

$$V_{oc} = S\Delta T \quad (1)$$

The Peltier effect states that when an electric current, I , passed through a junction of two dissimilar materials, heat, P , is evolved or absorbed at the junction:

$$P = \pi I = SI\Delta T_j \quad (2)$$

where π is the Peltier coefficient, and T_j is the junction temperature.

Two other and very important phenomena observed in TE materials are Joule heating effect and the Thomson effect [20]. In Joule heating, heat is generated due to the collision of charge carriers with the atoms or molecules of materials also known as resistive heating, $H = I^2R$. Thomson effect is defined as the reversible emergence or absorption of heat, T_T , when an electric current and temperature gradient exist simultaneously in TE materials forming an electrical circuit:

$$T_T = \tau I \Delta T \quad (3)$$

where τ is the Thomson coefficient and defined:

$$\tau = T_{avg} \frac{dS}{dT} \quad (4)$$

where $T_{ave} = (T_h + T_c)/2$ is the average temperature across the junction. Since the Thomson effect is lesser than the Joule heating effect, it is thus ignored in literature much of the time. The mathematical model used in this article also does not consider its influence.

Typically, TE devices consist of two materials, one of which is *n*-type and other is *p*-type. Both these materials are connected electrically in series and thermally in a parallel configuration to form a junction [21]. The electrical voltage is generated whenever the temperature gradient is present across the *p-n* junction [10, 22]. The efficiency of the thermoelectric modules (TEM) depends directly on the Carnot efficiency. If the temperature gradient, ΔT , is more, the conversion efficiency of the TEM would also be higher. Mostly, the thermoelectric generators (TEG) operate with a 20% Carnot efficiency. The efficiency of two different TEG at same temperature gradient depends upon a dimensionless material property called the TE figure of merit, ZT , given in eq. (1) [23]. Currently, the best available TE material has ZT value of 1. It is defined in mathematical terms as:

$$ZT = \frac{S^2 \sigma T}{\kappa_e + \kappa_l} \quad (5)$$

where σ is the electrical conductivity, κ_e – the electronic thermal conductivity, κ_l – the lattice thermal conductivity, and T – the absolute temperature.

Although TEG are less efficient than other traditional means of generating electricity, they are an active area of research worldwide because the exhaust from any power generating medium, such as IC engines, has virtually zero cost [24]. So, harvesting useful energy from waste heat is more appropriate for anyone rather than consuming some more fuel to meet the requirements [25, 26]. Large multinational automotive companies such as BMW, Ford, Renault, and Honda have shown their interests to develop the TEG system for the automotive applications to recover waste heat of the engine. However, this technical approach still is in concept stages. The BMW system exploited high temperature TEG to produce a power of 750 W [27]. The Ford system utilized small parallel channels covered with TE materials in the passage of exhaust gasses. The power produced in this system was 400 W [28]. The modelled system by Renault produced an electrical power of 1.01 kW [29]. The Honda system also used a heat exchanger (HEX) and TEM to produce a power of approximately 500 W [30]. They claimed 3% reduction of total fuel consumption. Nissan created the first TEG system for automotive applications based on Si-Ge in 1998 [31]. Moreover, in 2004, an efficient TE power generation system was built by bell solid-state TE including Marlow industries, Visteon, and BMW to recuperate waste thermal energy in passenger vehicles [27]. Eddin *et al.* [32] conducted experimental research on the pulsation effect of an engine's exhaust gas on the output of a TEG. Work shows that an IC engine with a power of 50 kW will produce 1 kW of electrical power if it recovers 2% of its waste thermal energy, which is sufficient to remove the alternator of that engine [12]. Liu *et al.* [33] experimented a TEG system on a vehicle called *Warrior* with a separate cooling system and maximum power output was 944 W.

In current work, we present a model for recovering the waste heat of an IC engine of 1.5 liters, using Na-K co-doped polycrystalline tin selenide (SnSe) TE material based modules. The model consists of an octagonal HEX on which 7 TEM can be mounted on 1/8th part and which can accommodate a total of 56 TEM on all sides. All the performance parameters like electrical voltage, current, power, and efficiency are plotted for one TEM. The transient response of total electrical power is plotted that we estimate to recover from the engine's exhaust. At normal conditions with an exhaust flow rate of 48 g/s using a SnSe based TEG, the system

can generate 477 W of electrical power. The current work provides an inexpensive alternative to the most popular TE material bismuth telluride Bi_2Te_3 for waste heat recovery. To offset the higher cost SnSe is a viable option having high power factor $492 \mu\text{W}/\text{mK}^2$, very low thermal conductivity and low cost comparatively.

Methodology to improve ZT

The literature has revealed that the power conversion efficiency of TE material is directly related to the dimensionless number called the figure of merit, ZT . The materials with

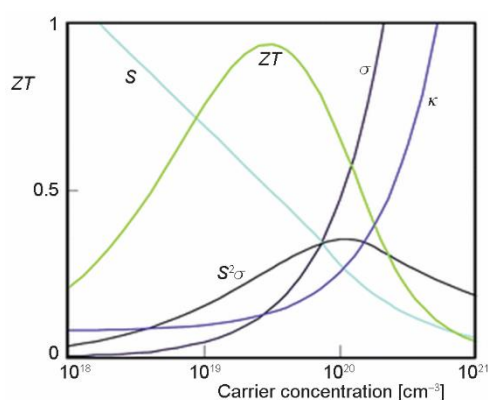


Figure 1. Interdependence of Seebeck coefficient, S , electrical conductivity, σ , power factor, $S^2\sigma$, thermal conductivity, κ , for a bulk material

high ZT will have a high Seebeck coefficient, high electrical conductivity and low thermal conductivity at simultaneously. In low charge carrier concentrations such as semiconductors or insulators, a strong Seebeck coefficient occurs, and high electrical conductivity is found in high charge carrier concentrations, *i. e.* in metals. Thus, somewhere in the center of metals and semiconductors, the TE power factor, $S^2\sigma$, maximizes [34]. Moreover, there is also an increase in thermal conductivity at high electrical conductivity, which eventually decreases the ZT as well as the conversion efficiency as shown in fig. 1 [35]. Consequently, a balance is formed between these three incompatible features and an optimum ZT value is achieved.

Mathematically, Seebeck coefficient is related to charge carrier concentration:

$$S = \frac{8\pi^2 k_B^2}{3eh^2} m^* T \left(\frac{\pi}{3n} \right)^{2/3} \quad (6)$$

where k_B is the Boltzmann constant, e – the charge on a carrier, h – the Plank's constant, m^* – the effective mass of the charge carrier, and n – is the concentration of the carriers. Similarly, electrical conductivity is also related to carrier concentration:

$$\sigma = ne\mu \quad (7)$$

where μ is carrier mobility. Typically, effective TE materials are found in a region where carrier concentration is 10^{19} - 10^{20} cm^{-3} which is in semiconductors. A heavily doped semiconductor of either n - or p -type is selected to ensure that the Seebeck coefficient is high, because semiconductors with both types result in the exact reverse Seebeck coefficient and therefore low power factor, $S^2\sigma$, is achieved. Moreover, it should also have a suitable energy bandgap ($<1 \text{ eV}$ mostly) with high carrier mobility to enhance electrical conductivity [34]. It is clear that to disassociate thermal conductivity, κ , including its both terms electronic, κ_e , and lattice, κ_l , and electronic properties, *i. e.*, electrical conductivity, σ , and Seebeck coefficient, S , figure of merit, ZT , can be increased.

Similarly, low thermal conductivity is required of an operating TE material. These materials' thermal conductivity is divided into two parts: electronic thermal conductivity, κ_e , and lattice thermal conductivity, κ_l , electronic thermal conductivity is associated with the heat transported by the charge carriers (electrons and holes) and lattice conductivity arises due to

heat transferred due to phonons travelling through the lattice. According to the Wiedemann-Franz law:

$$\kappa_e = L\sigma T \quad (8)$$

where L is the Lorenz number. It is clear from eq. (8) that electronic thermal conductivity is directly related to electrical conductivity, therefore to reduce electronic thermal conductivity will not be a suitable option as it will decrease electrical conductivity and has little or no increase in ZT . Lattice thermal conductivity is defined by the following relationship:

$$\kappa_l = \frac{1}{3(C_v v_s \lambda_{ph})} \quad (9)$$

where C_v is the heat capacity, v_s – the velocity of sound, and λ_{ph} – the phonon mean free path.

It is revealed from the literature that ZT can only be improved by decreasing the lattice thermal conductivity. There are two primary techniques used for decreasing the lattice thermal conductivity that goes in favor of ZT and ultimately power conversion efficiency of TEM. The first is *phonon glass electron crystal*, which recommends that the best TE material should have thermal conductivity like glass and electrical conductivity like crystal [36]. The material with complex crystal structure where atoms or molecules of heavy element act as phonon scattering centers and try to push back these thermal energy-carrying phonons as shown in fig. 2 [37].

The other technique is to nanostructure the TE materials. Through nanostructuring density of states is increased employing quantum confinement near the Fermi level which eventually increases the thermopower [35, 38]. Apart from this, as mean free path of electrons is much shorter as compared to phonons, so phonons are scattered back due to its large mean free path and greater density of interfaces of nanostructured material. Hence, this method reduces the thermal conductivity of material while keeping charge carriers in conduction.

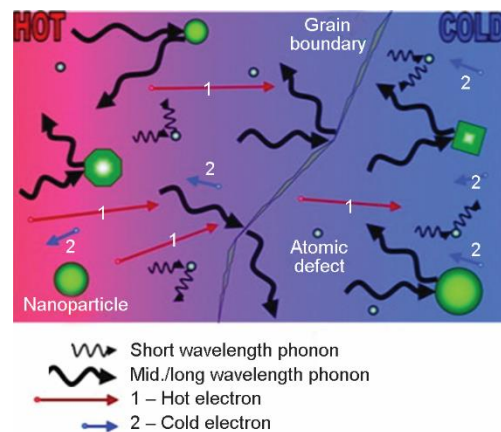


Figure 2. Illustration of phonons scattering by rattlers, nanoparticles, and grain boundaries in a TE material

Materials and methods

Modelling the engine exhaust system

In this simulation, an engine exhaust system in MATLAB/SIMULINK environment was modelled in the Simscape language as shown in fig. 3. The software provides fairly simple building blocks for modelling a physical system. In this model, the first heat was transferred from the exhaust gasses to a pipe utilizing heat transfer mechanism called convection, which was then conducted through the exhaust pipe to the hot side of TEM, finally being used by electrical power generation system. On the other hand, part of total energy was conducted again through TEM, that being further convected in the environment or cooling medium, which is not shown here for the sake of simplicity of the model. The value of the convective heat

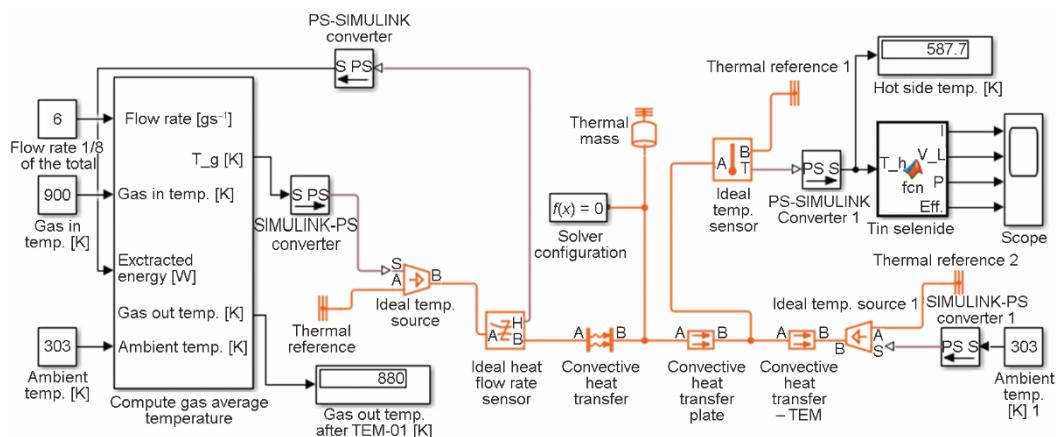


Figure 3. Physical model of engine's exhaust system on Simscape in MATLAB/SIMULINK environment and MATLAB function block containing mathematical model for one TEM of tin Selenide (SnSe) based material

transfer coefficient, h_c , used in this simulation between exhaust gasses and the internal surface of the HEx was $100 \text{ W/m}^2\text{K}^1$. In this model, one side of TEM was attached directly to the exhaust pipe having temperature 500-600 K almost and the other side remained at a constant temperature of 303 K. The mathematical model was developed using MATLAB for one module used in its original form in the SIMULINK environment. As the temperature gradient developed across the two sides of TEM, a transient signal of electrical voltage was observed. Similarly, all the other performance parameters were plotted against time as exhaust gasses flow through the exhaust pipe.

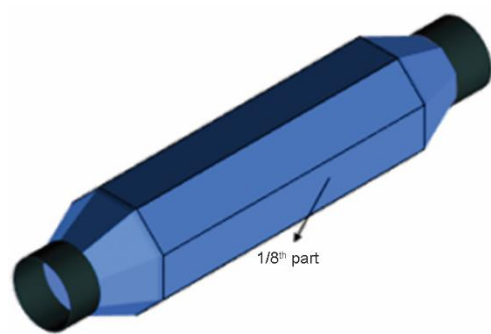


Figure 4. Octagonal HEx on the exhaust pipe for TEM mounting

was higher than the second one, similarly, this behavior was found in all the modules positioned in the longitudinal direction of the pipe, as some portion of the gas entropy was transformed into electrical power by each module. One assumption was made in this simulation that all sides of HEx uncovered by TEM were insulated and that there were no heat losses to the environment through these sides.

The HEx for this simulation was supposed to be an octagonal in shape as shown in fig. 4, where we were able to mount 56 TEM with dimensions of the each TEM being $56 \times 56 \times 4 \text{ mm}$. In order to increase the internal coefficient of convective heat transfer, this octagonal pipe may be equipped with an exhaust air deflector at the center which pushes the air towards the top wall of the HEx. For convenience, $1/8^{\text{th}}$ portion of this model was used for simulation instead of using the entire HEx. The temperature profile will be the same on all other faces due to symmetry so that the power output will also be the same. It was observed that the temperature on the hot side of the first module mounted on the exhaust pipe

Mathematical modelling of TE module

Mathematical model of the TEM is further categorized into electrical and thermal behaviors. The equations of these two responses were fed into MATLAB/SIMULINK for just one TEM and the response of different performance parameters was plotted. The power produced by one TEM is integrated to all other modules operating at same conditions.

Electrical behavior

The steady-state electrical parameters, *i. e.*, current, voltage, and power, form essentially linear relationships at constant temperature difference retained over a TEG, such that the electrical counterpart can be modelled as a DC source in series with internal resistance to a first approximation. The electrical current and voltage are expressed:

$$I = \frac{n_t S (T_h - T_c)}{R_L + R_{in}} \quad (10)$$

$$V = n_t [S (T_h - T_c) - I R_{in}] \quad (11)$$

where n_t is the number of thermocouples in one module, R_{in} – the internal resistance, and R_L – the load resistance. By choosing materials with higher electrical conductivity, reducing the leg length and increasing the cross-sectional area of thermocouples during processing, we aim to reduce the internal resistance, R_{in} , of TEM in order to achieve better performance [39].

Thermal behavior

In the thermal behavior of a TEG heat flow rate based on the given temperature gradient is calculated at both sides. Heat flow rate is a combination of Peltier heat, Fourier heat from one side to the other, and Joule heat at each side [40]. For these three categories, the heat flow rates on both sides are given:

$$Q_h = S I T_h + K (T_h - T_c) - 0.5 I^2 R_{in} \quad (12)$$

$$Q_c = S I T_c + K (T_h - T_c) - 0.5 I^2 R_{in} \quad (13)$$

where K is the thermal conductance. The difference between these two flow rates is equal to the electrical power output:

$$P_{out} = Q_h - Q_c = V I \quad (14)$$

Finally, the power conversion efficiency of TEM is the ratio between electrical output power to the input heat flow rate. Thermal conductivity should be minimal in order to achieve higher conversion efficiency:

$$\eta = \frac{P_{out}}{Q_h} \quad (15)$$

Results and discussion

Variation of TEM performance parameters

All performance parameters of the TEM are influenced by two variables: one is TEM hot side temperature, T_h , and the other is load resistance, R_L .

Effect of hot side temperature

The effect of TEM hot side temperature on the output electrical voltage, current and efficiency is linear. So, all these parameters increase linearly with the increase in temperature.

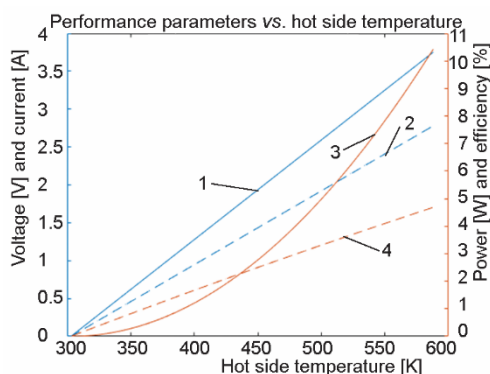


Figure 5. Variation of TEM performance parameters with its hot side temperature; TEM-01 performance parameters: 1 – voltage, 2 – current, 3 – power, 4 – efficiency

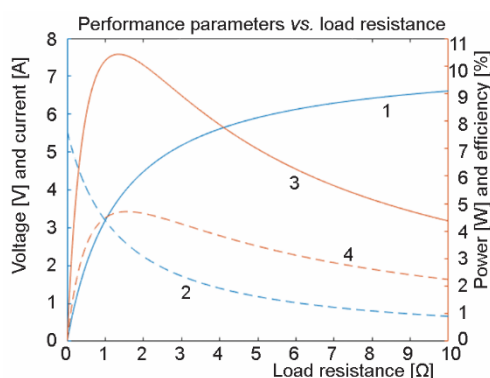


Figure 6. Variation of TEM performance parameters with its load resistance; TEM-01 performance parameters: 1 – voltage, 2 – current, 3 – power, 4 – efficiency

5.56 A, occurred at zero load resistance. Similarly, we got the maximum value of voltage called open circuit voltage at the infinite load resistance or at zero current. An open circuit voltage of 7.5 V was achieved from one TEM in this work. As the maximum load resistance of 10 Ω was taken for one TEM, so a load voltage value was 6.61 V with a very minute current flow of 0.66 A across this resistance.

The other aspect of identifying how the performance parameters of TEM are interrelated to each other is to see how they are changing their values concerning another specific parameter. Here, the graph between the electrical current flowing through the external circuit of only one TEM is plotted against voltage, power, and efficiency. When the current begins to

While the output power of the module increases parabolically with the temperature as shown in fig. 5. The maximum power of TEM-01 achieved was 10.4 W at 588 K hot side temperature. The maximum power conversion efficiency of TEM-01 achieved was 4.7% at the maximum hot side temperature which is 588 K in this case. As we move longitudinally on the HEX, efficiency of the respective TEM decreases because of decrease in hot side temperature.

Effect of load resistance

The behavior of performance parameters as the load resistance changes is quite different from the previous case. The output power increases gradually up to a specific ratio ($m = R_L/R_{in}$) of load and internal resistances. After that specific ratio its value starts to decrease. It was found that maximum output power occurs at $m = 1$, or $R_L = R_{in}$ called matched load power. On the other hand, power conversion efficiency maximizes at an optimal load condition [41], which is $m_{opt} = 1.14$, or $R_L = 1.14R_{in}$ for this SnSe based TEM, given as:

$$m_{opt} = \frac{R_L}{R_{in}} = (1 + ZT_{ave})^{0.5} \quad (16)$$

The other two parameters, load voltage and current increase and decrease respectively, with the increase in load resistance as shown in fig. 6. The load resistance, R_L , was varied from 0-10 Ω in this simulation. The maximum value of electrical current called short circuit current was

flow, the voltage decreases. We also observe a symmetrical curve of power and efficiency almost halfway through the short circuit current. Note, the peak points of these two curves occur at two different currents, as seen in fig. 7.

Transient variation of TEM hot side temperature and performance parameters

The temperature of the hot side of the TEM installed directly to the exhaust pipe increased as exhaust gasses started to flow. In this simulation, the flow rate of the exhaust gasses remained constant (48 g/s), which corresponds to 1.5 liters automotive IC engine in normal operating conditions. The exhaust gasses were circulated at three different inlet temperatures to the HEx. However, the transient response of TEM performance parameters was plotted at the exhaust gasses inlet temperature of 900 K. It can be noticed from the graph in fig. 8, that the hot side temperature of the very first TEM is more as compared to the last one because of the conversion of heat into electricity by the preceding TEM. The maximum hot-side temperature of the first TEM achieved was almost 588 K after 600 seconds while it was 534 K for the last TEM.

All the performance parameters of the TEM vary transiently in a same manner as the temperature of the hot side of TEM changes with respect to time as shown in fig. 9. In this work, the simulation time was set to 600 seconds and at this time all these parameters approached to their peak value and came in steady-state in the next interval after 600 seconds. The maximum value of each parameter occurred at the maximum hot side temperature on the respective TEM.

System total output power

The system was consisted of an octagonal HEx containing a total of 56 TEM, eight TEM located radially and seven TEM in the longitudinal direction up to a length of 400 mm. A temperature gradient was developed across all the TEM as the exhaust gasses started to flow. The power produced by the TEM mounted in the octagonal HEx radial direction in one set was the same, but as we traverse in the longitudinal direction, it continually decreased due to the reduction in hot side temperature. The following graph shows the power trend regarding simulation time at three different exhaust gas temperatures. The transient response of system total output power is plotted in fig. 10, at three different exhaust gas temperatures. It can be seen that the electrical power increases with the simulation time which is kept 600 seconds in this work. After that time there is insignificant or no transient increase in power and we say the system has come to a steady-state.

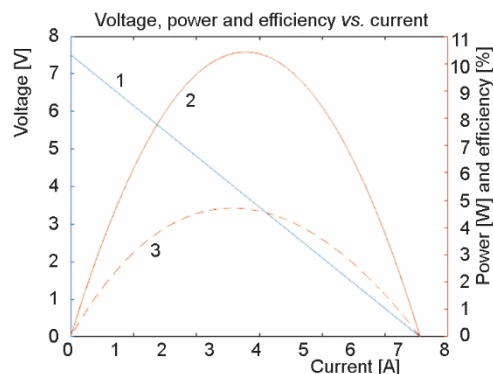


Figure 7. Interdependence of TEM different performance parameters; 1 – TEM-01 voltage, 2 – TEM-01 power, 3 – TEM-01 efficiency

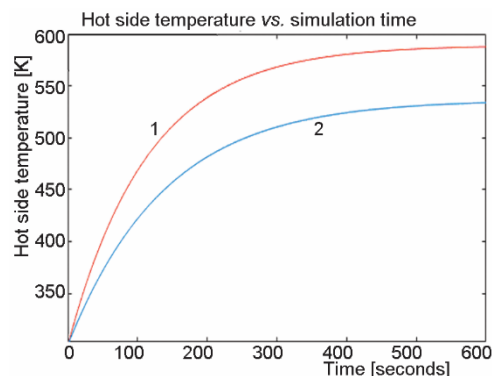


Figure 8. Transient variation of TEM hot side temperature; 1 – TEM-01 hot side temperature, 2 – TEM-07 hot side temperature

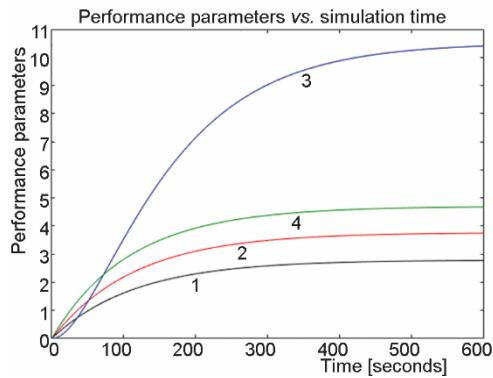


Figure 9. Transient variation TEM performance parameters; TEM-01 performance parameters:
1 – current, 2 – voltage, 3 – power, 4 – efficiency

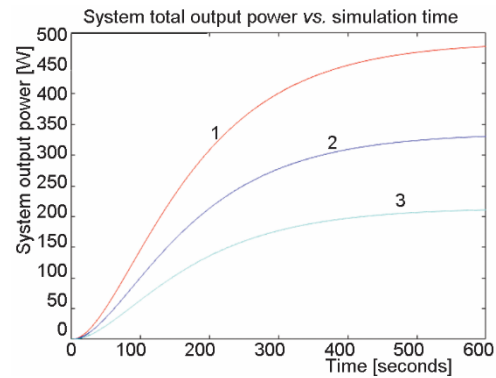


Figure 10. Transient variation of system total output power at three different exhaust gas temperatures; 1 – 900 K, 2 – 800 K, 3 – 700 K

Table 1 clearly demonstrates the electrical power produced by different sets of TEM mounted in radial direction of the octagonal HEx at three different temperatures of the exhaust gasses. It can be noticed from the table that the power generated by each TEM mounted on 1/8th part of HEx is multiplied by a factor of 8 in order to get total power. It can also be seen that electrical power generated by first collection of 8 TEM is greater in each case than the next coming sets. The total electrical power produced by this TEG system is 477 W when exhaust gas has temperature of 900 K at the inlet of HEx. It is reduced to 331 W and 211 W, as the exhaust gasses inlet temperature decrease to 800 K and 700 K respectively.

Table 1. Total power generated at three different exhaust gas inlet temperatures to the HEx

TEM at the HEx	P_{out} at 700 K [W]	P_{out} at 800 K [W]	P_{out} at 900 K [W]
TEM-01×8	36.8	57.6	83.2
TEM-02×8	34.4	53.8	77.6
TEM-03×8	32.0	50.4	72.4
TEM-04×8	29.8	46.8	67.5
TEM-05×8	27.8	43.6	63.0
TEM-06×8	26.0	40.8	58.6
TEM-07×8	24.2	38.0	54.7
Total 56 TEM	211	331	477

Conclusion

The potential of TE material based on polycrystalline tin-selenide, SnSe, for the recovery of automobile waste heat is investigated in this work. The introduction of co-doped rattlers (Na, K), and other intentionally introduced atomic scale structural defects because of phonons scattering, the selected material has a high TE power factor, $S^2\sigma$, and low thermal conductivity of the lattice, which improves its power conversion efficiency. The simulation model consists of an octagonal HEx on which 56 TEM are installed. At an inlet temperature of

900 K of exhaust gas to the HEx, the maximum electrical power produced by the very first and last TEM installed on it in the longitudinal direction, is 10.4 and 6.84 W, respectively, and the total TEG system has the capacity to produce 477 W under these operating conditions. The results of this work will pave the way for exploring new TE materials with better and more efficient performance and low-cost recovery of waste heat from IC engines. The present method can be extended to other waste heat recovery mechanisms using any suitable TE material.

Nomenclature

C_v – heat capacity, [JK⁻¹]
 e – charge, [C]
 h – Plank constant, [Js]
 K – thermal conductance, [WK⁻¹]
 k_B – Boltzmann constant, [JK⁻¹]
 L – Lorenz number, [W Ω K⁻²]
 m^* – effective mass, [kg]
 n – charge concentration, [cm⁻³]
 n_t – number of thermocouples
 P – Peltier heat, [J]
 P_{out} – output electrical power, [W]
 Q_c – heat flow rate at cold side, [Js⁻¹]
 Q_h – heat flow rate at hot side, [Js⁻¹]
 R_{in} – internal resistance, [Ω]
 R_L – load resistance, [Ω]
 S – Seebeck coefficient, [VK⁻¹]
 T – absolute temperature, [K]
 T_c – cold side temperature, [K]
 T_h – hot side temperature, [K]
 T_j – junction temperature, [K]
 T_r – Thomson heat, [J]

V_{oc} – open circuit voltage, [V]
 ZT – figure of merit
 ΔT – temperature gradient, [K]

Greek symbols

η – power conversion efficiency
 κ – thermal conductivity, [Wm⁻¹K⁻¹]
 κ_e – electronic thermal conductivity, [Wm⁻¹K⁻¹]
 κ_l – lattice thermal conductivity, [Wm⁻¹K⁻¹]
 λ_{ph} – phonon mean free path, [m]
 μ – carrier mobility, [m²V⁻¹s⁻¹]
 v_s – speed of sound, [ms⁻¹]
 π – Peltier coefficient, [V]
 σ – electrical conductivity, [Sm⁻¹]
 τ – Thomson coefficient, [VK⁻¹]

Abbreviations

HEx – heat exchanger
 TEG – thermoelectric generator
 TEM – thermoelectric module

References

- [1] Cao, Q., et al., Performance Enhancement of Heat Pipes Assisted Thermoelectric Generator for Automobile Exhaust Heat Recovery, *Appl. Therm. Eng.*, 130 (2018), Feb., pp. 1472-1479
- [2] Karthikeyan, B., et al., Exhaust Energy Recovery Using Thermoelectric Power Generation from a Thermally Insulated Diesel Engine, *Int. J. green energy*, 10 (2013), 10, pp. 1056-1071
- [3] Elsheikh, M. H., et al., A Review on Thermoelectric Renewable Energy: Principle Parameters that Affect their Performance, *Renew. Sustain. energy Rev.*, 30 (2014), Feb., pp. 337-355
- [4] Dolz, V., et al., HD Diesel Engine Equipped with a Bottoming Rankine Cycle as a Waste Heat Recovery System. Part 1: Study and Analysis Of The Waste Heat Energy, *Appl. Therm. Eng.*, 36 (2012), Apr., pp. 269-278
- [5] Shu, G., et al., Experimental Comparison of R123 and R245fa as Working Fluids for Waste Heat Recovery from Heavy-Duty Diesel Engine, *Energy*, 115 (2016), 1, pp. 756-769
- [6] Jorge, V., et al., State of the Art of Thermoelectric Generators Based on Heat Recovered from the Exhaust Gases of Automobiles, *Proceedings, 7th European Workshop on Thermoelectrics*, Pamplona, Spain, 2002
- [7] Hountalas, D. T., et al., Improvement of Bottoming Cycle Efficiency and Heat Rejection dor HD Truck Applications by Utilization of EGR and CAC Heat, *Energy Convers. Manag.*, 53 (2012), 1, pp. 19-32
- [8] Noor, A. M., et al., Waste Heat Recovery Technologies In Turbocharged Automotive Engine – A Review, *J. Mod. Sci. Technol.*, 2 (2014), 1, pp. 108-119
- [9] Shi, R., et al., System Design and Control for Waste Heat Recovery of Automotive Engines Based on Organic Rankine Cycle, *Energy*, 102 (2016), May, pp. 276-286
- [10] LeBlanc, S., Thermoelectric Generators: Linking Material Properties and Systems Engineering for Waste Heat Recovery Applications, *Sustain. Mater. Technol.*, 1 (2014), Dec., pp. 26-35
- [11] Sharma, S., et al., A Review of Thermoelectric Devices for Cooling Applications, *Int. J. green energy*, 11 (2014), 9, pp. 899-909

- [12] Kutt, L., Lehtonen, M., Automotive Waste Heat Harvesting for Electricity Generation Using Thermoelectric Systems – An Overview, *Proceedings, IEEE 5th International Conference on Power Engineering, Energy and Electrical Drives (Powereng)*, Riga, Latvia, 2015, pp. 55-62
- [13] Temizer, I., *et al.*, Analysis of an Automotive Thermoelectric Generator on a Gasoline Engine, *Thermal Science*, 24 (2019), 1, Part A, pp. 137-145
- [14] He, R., *et al.*, Studies on Mechanical Properties of Thermoelectric Materials by Nanoindentation, *Phys. status solidi*, 212 (2015), 10, pp. 2191-2195
- [15] Ge, Z.-H., *et al.*, Boosting the Thermoelectric Performance of (Na, K)-Codoped Polycrystalline SnSe by Synergistic Tailoring of the Band Structure and Atomic-Scale Defect Phonon Scattering, *J. Am. Chem. Soc.*, 139 (2017), 28, pp. 9714-9720
- [16] Saqr, K. M., Musa, M. N., Critical Review of Thermoelectrics in Modern Power Generation Applications, *Thermal Science*, 13 (2009), 3, pp. 165-174
- [17] LeBlanc, S., Thermoelectric Generators: Linking Material Properties and Systems Engineering for Waste Heat Recovery, *Sustainable Materials and Technologies*, 1-2 (2014), Dec., pp. 26-35
- [18] Jin, W., *et al.*, Exploring Peltier Effect in Organic Thermoelectric Films, *Nat. Commun.*, 9 (2018), 1, pp. 1-6
- [19] Rowe, D. M., *Thermoelectrics Handbook: Macro To Nano*, CRC press, Boca Raton, Fla., USA, 2018
- [20] Du, C.-Y., Wen, C.-D., Experimental Investigation and Numerical Analysis for One-Stage Thermoelectric Cooler Considering Thomson Effect, *Int. J. Heat Mass Transf.*, 54 (2011), 23-24, pp. 4875-4884
- [21] Dusastre, V., *Materials for Sustainable Energy: A Collection of Peer-Reviewed Research and Review Articles from Nature Publishing Group*, World Scientific, Singapore, 2011
- [22] Nikolić, R. H., *et al.*, Modeling of Thermoelectric Module Operation in Inhomogeneous Transient Temperature Field Using Finite Element Method, *Thermal Science*, 18 (2014), Suppl. 1, pp. S239-S250
- [23] Snyder, G. J., Snyder, A. H., Figure of Merit ZT of a Thermoelectric Device Defined from Materials Properties, *Energy Environ. Sci.*, 10 (2017), 11, pp. 2280-2283
- [24] Meng, J.-H., *et al.*, Performance Investigation and Design Optimization of a Thermoelectric Generator Applied in Automobile Exhaust Waste Heat Recovery, *Energy Convers. Manag.*, 120 (2016), July, pp. 71-80
- [25] Rodriguez, R., *et al.*, Review and Trends of Thermoelectric Generator Heat Recovery in Automotive Applications, *IEEE Trans. Veh. Technol.*, 68 (2019), 6, pp. 5366-5378
- [26] Xiao, G.-Q., Zhang, Z., Coupled Simulation of a Thermoelectric Generator Applied in Diesel Engine Exhaust Waste Heat Recovery, *Thermal Science*, 24 (2019), 1, Part A, pp. 281-292
- [27] LaGrandeur, J., *et al.*, Automotive Waste Heat Conversion to Electric Power Using Skutterudite, TAGS, PbTe and BiTe, *Proceedings, 25th International Conference on Thermoelectrics*, Vienna, Austria, 2006, pp. 343-348
- [28] Hussain, Q. E., *et al.*, Thermoelectric Exhaust Heat Recovery for Hybrid Vehicles, *SAE Int. J. Engines*, 2 (2009), 1, pp. 1132-1142
- [29] Espinosa, N., *et al.*, Modeling a Thermoelectric Generator Applied to Diesel Automotive Heat Recovery, *J. Electron. Mater.*, 39 (2010), 9, pp. 1446-1455
- [30] Mori, M., *et al.*, Simulation of Fuel Economy Effectiveness of Exhaust Heat Recovery System Using Thermoelectric Generator in a Series Hybrid, *SAE Int. J. Mater. Manuf.*, 4 (2011), 1, pp. 1268-1276
- [31] Ikoma, K., *et al.*, Thermoelectric Module and Generator for Gasoline Engine Vehicles, *Proceedings, 17th International Conference on Thermoelectrics. Proceedings ICT98* (Cat. No. 98TH8365), 1998, pp. 464-467
- [32] Eddine, A. N., *et al.*, Effect of Engine Exhaust Gas Pulsations on the Performance of a Thermoelectric Generator for Wasted Heat Recovery: An Experimental and Analytical Investigation, *Energy*, 162 (2018), Nov., pp. 715-727
- [33] Liu, X., *et al.*, Performance Analysis OF A Waste Heat Recovery Thermoelectric Generation System for Automotive Application, *Energy Convers. Manag.*, 90 (2015), Jan., pp. 121-127
- [34] Vaquero, P., Powell, A. V., Recent Developments in Nanostructured Materials for High-Performance Thermoelectrics, *J. Mater. Chem.*, 20 (2010), 43, pp. 9577-9584
- [35] Szczech, J. R., *et al.*, Enhancement of the Thermoelectric Properties in Nanoscale and Nanostructured Materials, *J. Mater. Chem.*, 21 (2011), 12, pp. 4037-4055
- [36] Slack, G. A., Rowe, D. M., *CRC Handbook of Thermoelectrics*, CRC press, Boca Raton, Fla, USA, 1995
- [37] Vineis, C. J., *et al.*, Nanostructured Thermoelectrics: Big Efficiency Gains from Small Features, *Adv. Mater.*, 22 (2010), 36, pp. 3970-3980

- [38] Rabari, R., *et al.*, Analysis of Combined Solar Photovoltaic-Nanostructured Thermoelectric Generator System, *Int. J. Green Energy*, 13 (2016), 11, pp. 1175-1184
- [39] Lineykin, S., Ben-Yaakov, S., Modeling and Analysis of Thermoelectric Modules, *IEEE Trans. Ind. Appl.*, 43 (2007), 2, pp. 505-512
- [40] Elarusi, A. H., *et al.*, Theoretical Approach to Predict the Performance of Thermoelectric Generator Modules, *J. Electron. Mater.*, 46 (2017), 2, pp. 872-881
- [41] Tsai, H.-L., Lin, J.-M., Model Building and Simulation of Thermoelectric Module Using Matlab/Simulink, *J. Electron. Mater.*, 39 (2010), 9, 2105